New Horizons in Earth Reinforcement – Otani, Miyata & Mukunoki (eds)

Full-scale behavior of a surface loaded geosynthetic reinforced tiered segmental retaining wall

C. Yoo, S.B. Kim & Y.H. Kim
Sungkyunkwan University, Suwon, Korea

ABSTRACT: This paper presents the results of a load test for a full-scale geosynthetic reinforced segmental retaining wall (GR-SRW) in a tiered arrangement. A four year old, 5 m high tiered SRW, originally constructed to investigate short and long term behavior, was load tested using a large precast concrete box culvert filled with ready mix concrete, simulating a surcharge loading condition of a GR-SRW in bridge abutment application. Measured items included horizontal displacement at the wall face and strains in the reinforcement. The measured results revealed that the GR-SRW's response was well within the serviceability limits and within the range of those predicted based on the current design guideline. Design implications and the findings from this study are discussed.

1 INTRODUCTION

The use of geosynthetic reinforced segmental retaining wall (GR-SRW) in both private and public sectors is increasing worldwide. Although the currently available limit equilibrium-based design approaches, such as NCMA (Collin, 1997) and FHWA (Elias and Christopher, 1997) design guidelines, are considered to be conservative on account of several assumptions regarding the wall behavior, much still needs to be investigated to bridge the gap between the theory and the practice. In addition, despite the fact that many geosynthetic reinforced soil walls have been safely constructed and are performing well to date, there are many areas that need in-depth studies to develop a more generalized design approach that will help safely construct GR-SRW systems under more aggressive and complex boundary conditions.

Recently GR-SRWs are frequently used in bridge construction, as the form of geosynthetic-reinforced soil (GRS) bridge-supporting structure (Lee and Wu 2004). The GRS bridge-supporting structure can be constructed using either rigid or flexible facings. A "rigid" facing is either precast or cast-in-place type while a "flexible" facing takes the form of wrapped geosynthetic sheets, segmental blocks, or gabions (Lee & Wu 2004). Lee & Wu (2004) synthesized measured data of four in-service GRS bridge abutments and six full-scale field experiments, and concluded that GRS bridge abutments with flexible facing are indeed a viable alternative to conventional bridge abutments.

A number of studies concerning GRS bridge-supporting structures with flexible facings are available, i.e., Mannsbart and Kropik (1996), Won et al. (1996), Wu et al. (2001), and Abu-Hejleh et al. (2000). Although these studies provided valuable information as to the performance of GRS-bridge-supporting structures with flexible facings, much still need to be investigated to better understand the response of GRS abutment to bridge loading.

In the present investigation, a four year old, 5 m high, two tier GR-SRW was load tested at Geotechnical Experimentation Site (GES) in Sungkyunkwan University, located in Suwon, Korea. A primary objective of the test was to evaluate the performance of a GR-SRW under a surcharge load, simulating a loading condition when used as a bridge abutment. This paper describes the test wall, the load test program, details of the observed performance, and finally, design implications.

2 DESIGN CONSIDERATION OF GR-SRW ABUTMENT

According to the FHWA design guideline, a GR-SRW bridge abutment can be designed as being a wall with surcharge load at the top of the wall. The internal stability calculations are performed by taking account of both vertical and horizontal components of the surcharge load. The reinforcement force T_i at ith level is computed based on the lateral pressure $\sigma_{H,i}$ and the tributary area $A_{t,i}$ as given in Eq. (1).

$$\sigma_{H,i} = K\left(\gamma z_i + \Delta\sigma_{V,i}\right) + \Delta\sigma_{h,i} \tag{1}$$

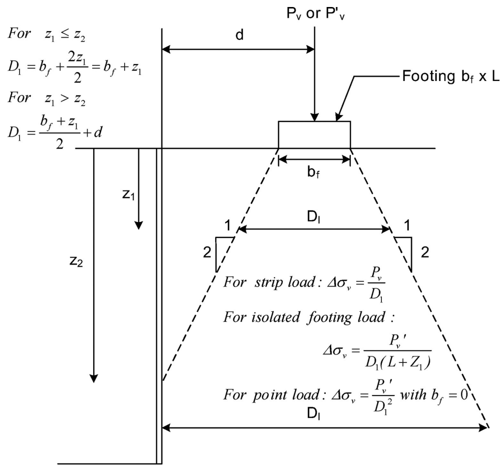

Figure 1. 2V:1H pyramid distribution.

where K is the lateral earth pressure coefficient, $\Delta\sigma_{V,i}$ is the increment of vertical stress due to the concentrated vertical surcharge assuming a 2V:1H pyramid distribution (Figure 1), $\Delta\sigma_{h,i}$ is the incremental horizontal stress due to the horizontal loads, and γz_i is the vertical stress at ith level.

3 WALL DESCRIPTION

3.1 *Site condition*

The ground under which the test wall was situated consists of approximately 3.0 m thick miscellaneous fill material including sand and gravel. Underlying the fill layer is a 3.0 to 4.0 m thick alluvial sandy clay deposit followed by a 6.0 to 8.0 m thick weathered granite residual soil overlying a slightly weathered granite rock stratum (Figure 2). Details of the site condition are given in Yoo & Jung (2004).

3.2 *Wall design and construction*

The wall was originally constructed in 2002 in order to investigate the short and long term performance of a two tier GR-SRW. The measured performance during construction based on an extensive field instrumentation has been reported in Yoo & Jung (2004). A brief discussion of the wall design and construction is given in this section.

The test wall had an exposed height of 5 m and consisted of two tiers, i.e., a 3.4 m high lower tier and a 2.2 m high upper tier as illustrated in Figure 3. The upper and lower tiers had no pre-batter angle and the face of the upper tier was 1.0 m away from the lower tier face, thus giving an offset distance of 1.0 m. As seen in Figure 4, eleven layers of PET reinforcement, having a

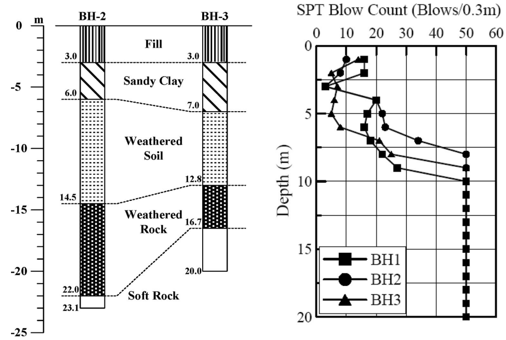

(a) soil profile (b) SPT results

Figure 2. Foundation soil profile & SPT blow counts for GES.

Figure 3. Photo of load test.

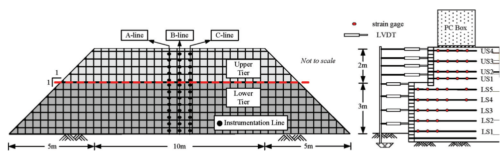

Figure 4. Schematic view of load test setup.

tensile strength of 55 kN/m at strain of 12.5% with an average axial stiffness of J = 500 kN/m, were placed at a maximum vertical spacing of 0.6 m. For each tier, the reinforcement length ratio with respect to the respective tier height was kept constant at 1.0. Note that the facing blocks are 450 × 330 mm in plan × 200 mm in height, having a compressive strength of 21 MPa with a maximum water absorption of 6∼8% for standard weight aggregates. Shear transfer between the blocks is developed primarily through shear keys formed on each block. Note that no provision was made for any future surcharge loading in terms of the internal and external stability at the time of wall design and construction.

Table 1. Results of internal stability calculations.

		Internal stability			
		FS_{to}		FS_{po}	
Layer	Elev. (m)	NCMA	FHWA	NCMA	FHWA
B1	0.2	1.59	1.32	33.21	28.07
LS1	0.6	1.38	1.15	24.28	21.30
LS2	1.2	1.31	1.09	17.37	15.84
LS3	1.8	1.53	1.27	14.50	14.12
LS4	2.4	1.84	1.52	11.64	12.40
LS5	3.0	2.30	1.66	8.78	9.35
US1	3.6	3.68	3.8	17.82	13.44
US2	4.0	4.78	4.05	15.53	9.72
US3	4.6	6.90	5.70	10.18	6.09
US4	5.2	33.12	21.89	8.55	4.19

A weathered granite soil, classified as SW-SM according to Unified Soil Classification System (USCS) was used as select fill and compacted to 95% of its maximum unit weight to create both the reinforced and retained zones. The estimated internal friction angle using a large scale direct shear test at a density corresponding to the as-compacted state was approximately 35° with a cohesion of 10 kPa. The results of the internal and external calculations for as-built design according to the NCMA and FHWA design guidelines are given Table 1.

4 LOAD TEST

4.1 *Test setup*

The load test was carried out in August of 2006, four years after the wall construction. The load was applied using a precast concrete box frame (2.4 m × 2.4 m in plan) for sewage drainage together with ready mixed concrete and a steel frame, totaling approximately 348 kN (Figure 3). As seen in Figure 4 showing the test setup, the concrete box was placed 0.5 m away from the upper tier facing units. The applied load exerted approximately 62 kPa of vertical pressure at the top of the wall. Such a pressure is within the typical design pressure for single span bridge deck when a GR-SRW is used to as a bridge abutment, and thus can be considered as a working load. During the test the load was applied in five increments by controlling the amount of remicon put into the concrete box as summarized in Table 2. During the test, the test load was applied in 20 kN increments by pouring in the remicon of 3∼4 m^3 in the concrete box. For each load increment a sufficient amount of time was allowed for the wall displacement to stabilize before a next load increment. A total of five and a half hours were required to complete the test.

Table 2. Summary of load application process.

Step	Incremental load (kN)	Cumulative load (kN)	% of total load	Loading description
1	78	78	22.4	placement of concrete box
2	69	147	42.2	1st Remicon of 3 m^3
3	69	216	62.1	2nd Remicon of 3 m^3
4	92	308	88.5	3rd Remicon of 4 m^3
5	40	348	100.0	Steel frame
6	−40	308	88.5	Unload steel frame

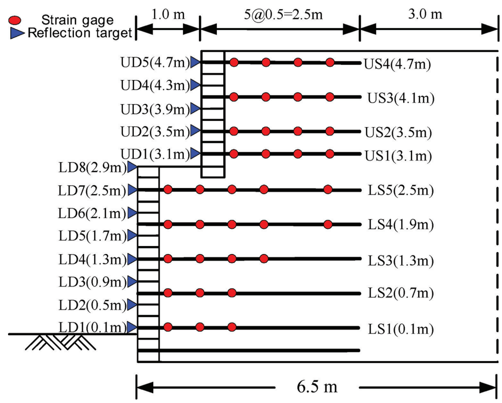

Figure 5. Instrumentation layout.

4.2 *Instrumentation*

The response of the test wall to the surface loading was evaluated in terms of the wall facing displacement and the reinforcement strains. Figure 5 shows the schematic layout of instrumentation. The wall facing displacement was measured by leveling using a 3D total station (MONMOS Model NEA2A) together with the reflection targets installed on the wall face. For redundancy of the wall facing displacement measurements eight potentiometers were additionally placed on a vertical row as shown in Figure 4.

Reinforcement strains were measured using strain gauges, high elongation bonded resistance strain gages, manufactured by Tokyo Sokki Kenyujo Company (Model YFLA-5-1L), that had survived at the time of the load test after their installation. Note that of the approximately 70% of xx strain gauges installed during construction had survived. The three instrument arrays for the leveling targets and the reinforcement strain measurements are shown in Figure 5. Table 3 summarizes the details of the instrumentation.

Table 3. Details on instruments.

Array/Instrumentation	Location
Array A, B, C	−1.0, 0, +1.0 from wall center line
Optical survey target on wall facing column	0.1, 1.5, 0.9, 1.3, 1.7, 2.1, 2.5, 2.9 3.1, 3.5, 3.9, 4.3, 4.7 m above wall base
Strain gage	0.5, 1.0, 1.5 m behind wall facing (LS1–LS3) 0.5, 1.0, 1.5, 2.5 m behind wall facing (LS4–LS5) 0.5, 1.0, 1.5, 2.5, 3.0 m behind wall facing (US1–US4)

5 RESULTS

5.1 *Lateral wall displacement*

Figure 6 shows the progressive development of wall displacements at the monitoring point. As seen in this figure, stepwise increases in the lateral wall displacements are evident due to the stepwise increase in the surcharge load. It is seen in Figure 6(a) only minimal displacements are measured in the lower tier at the final stage of the loading, showing a maximum of 0.5 mm. As expected, larger lateral displacements are measured in the upper tier with a maximum of 1.7 mm at the upper most measuring point, as shown in Figure 6(b). Such results are well reflected in the lateral wall displacement profiles at the final loading stage in Figure 7, in which a cantilever type movement prevails.

5.2 *Reinforcement strains*

The progressive development of strains in the reinforcement layers due to the surface loading is shown in Figure 8. No appreciable strains in layers LS1∼LS4 in the lower tier were recorded and therefore are not given here. The influence depth for the surface load can thus be inferred as being slightly larger than the upper tier height of 2 m. As seen for layer LS5 in Figure 8, a maximum strain of 0.05% was developed at the location close to the end of the layer with essentially negligible strains elsewhere. A decrease in strain of approximately 0.1% is noticed at the mid location of the layer (LS5), although the cause for such a trend is not immediately clear.

In the upper layers, as seen in Figure 9(a)∼9(c), stepwise increases in strains caused by the stepwise increase in the load are evident, showing a maximum strain of 0.1% occurring at the top layer US4. As one can expect, the absolute maximum increase in each layer increases with increasing the proximity to the load. Of interest trends in this figure are twofold. First, for each load increment a sharp increase in strain is noticed immediately after the load increment, followed

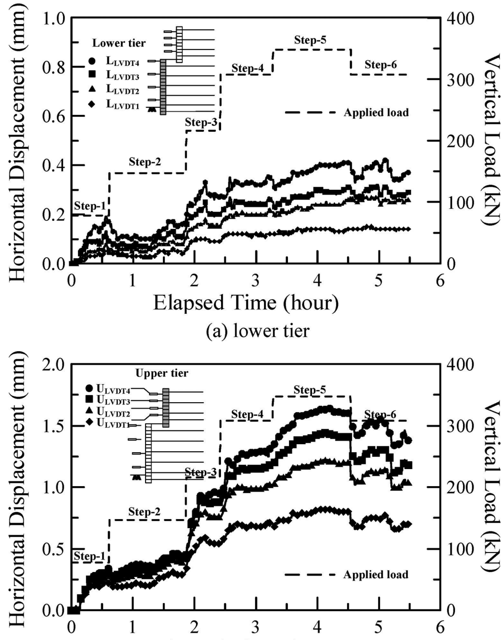

(a) lower tier

(b) upper tier

Figure 6. Progressive development of wall displacements at monitoring points.

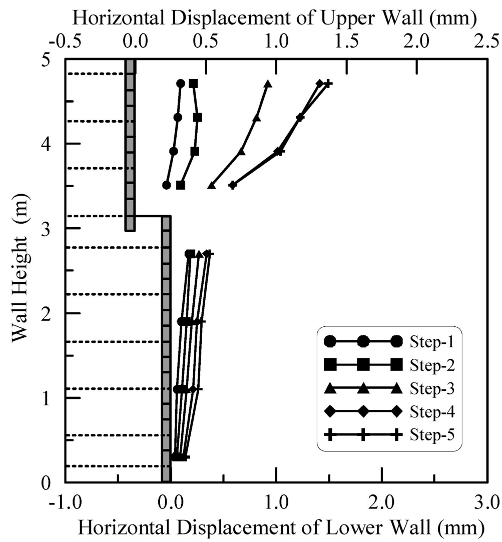

Figure 7. Wall displacement profiles at various loading stages.

by gradual convergence to a certain value. Note that such a trend is in fact similar to the observation in a sustained loading test on a reduced geosynthetic reinforced wall (Yoo et al., 2006). Another of interest

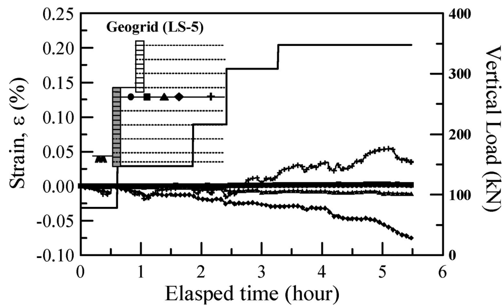

Figure 8. Progressive development of wall displacements at monitoring points (lower tier).

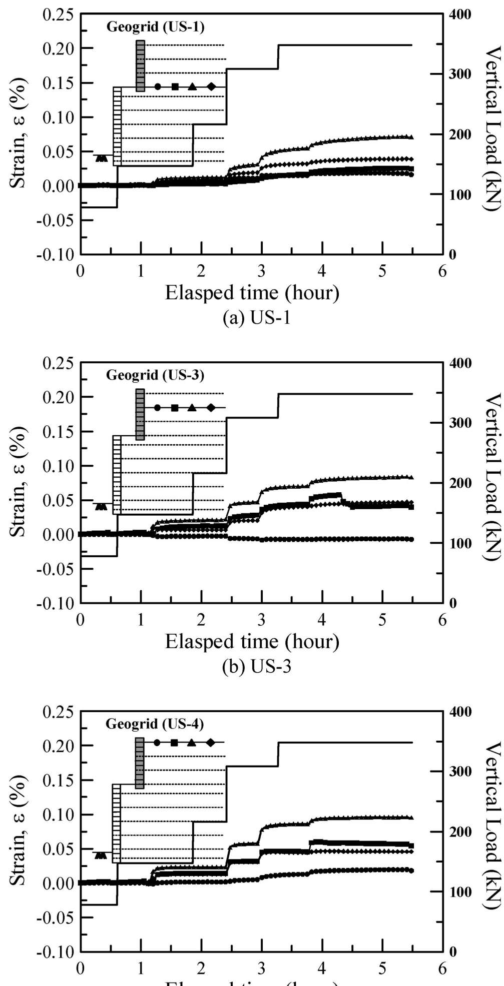

(a) US-1

(b) US-3

(c) US-4

Figure 9. Progressive development of wall displacements at monitoring points (upper tier).

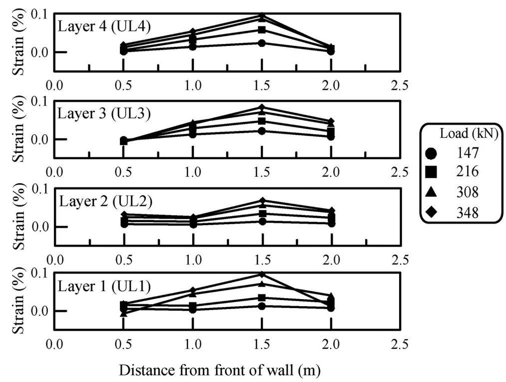

Figure 10. Reinforcement strain distributions for reinforcements in upper tier at final loading stage.

Table 4. ΔT according to FHWA design guideline.

Layer	h (m)	$\Delta\sigma_V$ (kPa)	$\Delta\sigma_H$ (kPa)	A_t (m^2)	ΔT (kN/m)
US4	4.7	48.01	14.4	0.6	8.6
US3	4.1	32.14	9.6	0.6	5.8
US2	3.5	23.01	6.9	0.5	3.5
US1	3.1	18.93	5.7	0.4	2.3
LS5	2.5	14.58	4.4	0.7	3.1
LS4	1.9	11.57	3.5	0.6	2.1
LS3	1.3	9.41	2.8	0.6	1.7
LS2	0.7	7.80	2.3	0.6	1.4
LS1	0.1	6.57	2.0	0.5	1.0

trend is that location of the largest strain increase for a given layer. As seen in these figures, a largest increase occurs approximately at the location 0.7 L from the wall facing for a given layer. Such a trend is well reflected in Figure 10 in which the reinforcement strain distribution for a given layer follows a concave-up shape showing a maximum strain at approximately 0.7 L from the wall facing, not directly under the loading center. The lateral wall yielding (displacement) may be attributed such a trend and therefore, a non-uniform strain increase along a layer should therefore be expected for a loading case similar to the one considered in this study.

Table 4 summarizes increases in the reinforcement forces ΔT computed according to the FHWA design guideline. The computed values in fact more than twice the measured values. This will be studied further in a future study.

In short, the surface loading of 60 kPa on a 1.5 m × 1.5 m loaded area induced reinforcement strains in the upper tier less than 0.1%, while negligible reinforcement strains were developed in the lower tier. These strain values are is well within the serviceability limits of the reinforcement. The calculation results based on the FHWA guideline yielded are however 50% larger than measured ones, suggesting some degree of conservatism in the current design approach. Further study is necessary in this area to further refine the calculation model adopted in the FHWA design guideline.

6 CONCLUSIONS

This paper presents the results of a load test of a full-scale geosynthetic reinforced segmental retaining wall (GR-SRW) in a tiered arrangement. A four year old, 5 m high tiered SRW, constructed to investigate short and long term behavior, was load tested using a large box culvert filled with ready mix concrete, simulating a loading condition of a SRW in bridge abutment application. Measured items included horizontal deformation at the wall face and strains in the reinforcement.

The measured results revealed that the SRW's response was well within the serviceability limits and within the range of those predicted based on the current design guideline. Also shown is that the calculation results based on the FHWA guideline yielded however 50% larger than measured ones, suggesting a conservatism in the current design guidelines. In short, the surcharge load of 348 kN did not significantly increase the wall performance in terms of the wall displacement and the reinforcement strains, although the surcharge load was not accounted for during design. Such a result demonstrates that a GR-SRW can be effectively used in surcharge loading situations.

ACKNOWLEDGEMENT

This work was supported by Grant No. R01-2004-000-10953-0 from the Basic Research Program of the Korea Science & Engineering Foundation. The financial support is gratefully acknowledged.

REFERENCES

Abu-Hejleh, N., Wang, T., Zornberg, J.G. 2000. Performance of geosynthetics-reinforced walls supporting bridge and approaching roadway structures. *ASCE Geotechnical Special Publication No. 103, Advances in Transportation and Geoenvironmental Systems using Geosynthetics*: 218–243.

Collin, J. 1997. Design Manual for Segmental Retaining Walls, 2nd Ed. NCMA, Virginia.

Elias, V. & Christopher, B.R. 1997. Mechanically Stabilized Earth Walls and Reinforced Soil Slopes, Design and Construction Guidelines. *FHWA Demonstration Project 82*, FHWA, Washington, DC, FHWA-SA-96-071.

Jappelli, R. & Marconi, N. 1997. Recommendations and prejudices in the realm of foundation engineering in Italy: A historical review. In Carlo Viggiani (ed.), *Geotechnical engineering for the preservation of monuments and historical sites*; *Proc. intern. symp., Napoli, 3–4 October 1996*. Rotterdam: Balkema.

Lee, K.Z.Z. & Wu, J.T.H. 2004. A synthesis of case histories on GRS bridge-supporting structures with flexible facing. *Geotextiles and Geomembranes*: Vol. 22, No. 4: 181–204.

Mannsbart, G. & Kropik, C. 1996. Nonwoven geotextile used for temporary reinforcement of a retaining structure under a railroad grack. In DeGroot, M.B., Hoedt, G., Termaat, R.J.(Eds.), *Geosynthetics: Applications, Design and Construction*: 121–124. Rotterdam: Balkema.

Won, G.W., Hull, T., De Ambrosis, L. 1996. Performance of a geosynthetics segmental block wall structure to support bridge abutments. In Ochiai, H., Yasufuku, N., Omine, K. (Eds.), *Earth Reinforcement*: Vol. 1. 543–548. Rotterdam: Balkema.

Wu, J.T.H., Ketchart, K., Adams, M. 2001. GRS bridge piers and abutments. Report FHWA-RD-00-038. FHWA, US Department of Transportion, 136pp.

Yoo, C. & Jung, H.S. 2004. Measured behavior of a geosynthetic-reinforced segmental retaining wall in a tiered configuration. *Geotextiles and Geomembranes*: Vol. 22, No. 5: 359–376.

Yoo, C., Kim, S.B., Kim, Y.H. 2006. Behavior of geosynthetic reinforced wall under sustained and cyclic loads – Reduced-scale model test. *Proc. Fall KGS Conference*: 24–25.